ly intact but delayed the peak of the second glimpse by 100 msec (Fig. 2f). Further dimming of the outline square (to an intensity level at which the square was still always detected but motor reaction times were slowed by 65 msec relative to the full-intensity square) greatly altered first glimpse responses (Fig. 2g). Interposing a bright masking field composed of a dense dot matrix between successive numeral frames also destroyed the first glimpse but left the second glimpse relatively intact. These two manipulations dissolved the perceptual glue (*16*) binding the outline square to the interior numeral.

In the case of the highlighted numeral target, when we randomly varied the intensity of all the other numerals from frame to frame, and we made the highlighted numeral only somewhat more intense than the strongest of its competitors (a signal-to-noise manipulation), the first glimpse remained intact, but the second glimpse was delayed by about 100 msec. Another factor, level of practice, had strong effects on second glimpse responses but almost no effect on first glimpse responses.

Late in the stimulus sequence, before a target had occurred, the instantaneous probability that a target would occur became much greater than early in the sequence. Correspondingly, the subjects' expectancy of a target increased as the end of the stimulus sequence was approached. Like motor-reaction times, second glimpse responses sped up with this increased expectancy; first glimpse responses were unaffected. Another form of expectancy occurred in mixed-list stimulus presentations when the subject did not know which target to expect: OS or HN. Compared with pure blocks of OS or HN trials, the second glimpse mixed-list responses were later in the numeral sequence; the first glimpse responses were unaffected by this form of stimulus uncertainty (Fig. 2h).

We also used an auditory click as the stimulus for triggering an attentional gate. The distribution of numerals reported in response to the click stimulus is shown in Fig. 2i. The cross-modality data showed an appreciable proportion of recalls of the numeral that preceded the target by 100 msec. These early recalled stimuli indicated that, in the absence of competing visual stimuli, there was some memory for visual stimuli that preceded the attention trigger; they also indicated that an intermodality attention shift could be extremely quick. The click procedure demonstrated the feasibility of directly measuring the gating of visual inputs by auditory signals, a critical feature of the partial report procedure for measuring visual very short term memory (*2*) and of the Reeves-Sperling theory of temporal order judgments (*1*).

Bimodal distributions of reports from a rapid numeral stream are explained in terms of two consecutive, partially overlapping attentive processes. A fast process (interpreted as a first glimpse by the subject) occurred automatically upon target detection and resulted in almost perfect recall of the target numeral as well as in occasional recall of a numeral immediately after the target. The automatic process was effortless, required no practice, and was virtually independent of task difficulty. For the subject to have recalled a numeral from the numeral stream in the automatic process required that his or her attention was not withdrawn to another location away from numerals (as in procedure 1) and that the target was sufficiently distinctive (for example, not too dim). With outline square targets (but not with highlighted numeral targets), the automatic process was destroyed by masking fields interposed between successive numeral frames.

An effortful, slow attentive process (interpreted as a second glimpse by the subject) mediated recall of numerals occurring more than 200 to 300 msec after the target. This was a controlled attentional process whose latency depended on factors that classically affect task difficulty: practice, expectation, stimulus probability in mixed-list designs, and target signal-to-noise ratio.

REFERENCES AND NOTES

1. A. Reeves and G. Sperling, *Psychol. Rev.* **93**, 180 (1986).
2. G. Sperling, *Psychol. Monogr.* **74**, No. 11 (whole No. 498) (1960).
3. M. Coltheart, *Percept. Psychophys.* **27**, 183 (1980).
4. G. M. Long, *Psychol. Bull.* **88**, 785 (1980).
5. M. L. Shaw and P. Shaw, *J. Exp. Psychol.: Human Percept. Perform.* **3**, 201 (1977).
6. J. A. Swets, in *Varieties of Attention*, R. Parasuraman and D. R. Davies, Eds. (Academic Press, New York, 1984), pp. 183–242.
7. D. E. Broadbent, *Psychol. Rev.* **64**, 205 (1957).
8. A. Treisman, *ibid.* **76**, 282 (1969).
9. R. M. Shiffrin, in *Stevens' Handbook of Experimental Psychology*, R. C. Atkinson, R. J. Herrnstein, G. Lindzey, R. D. Luce, Eds. (Wiley, New York, ed. 2, in press).
10. G. Sperling and B. A. Dosher, in *Handbook of Perception and Performance*. K. Boff, L. Kaufman, J. Thomas, Eds. (Wiley, New York, 1986), vol. 1, pp. 2.1–2.65.
11. E. Weichselgartner, thesis, New York University, (1984).
12. R. M. Shiffrin and W. Schneider, *Psychol. Rev.* **84**, 127 (1977).
13. G. Sperling and A. Reeves, in *Attention and Performance*, R. Nickerson, Ed. (Erlbaum, Hillsdale, NJ, 1980), vol. 8, pp. 347–360.
14. M. C. Potter and E. I. Levy, *J. Exp. Psychol.* **81**, 10 (1969).
15. G. Sperling, J. Budiansky, J. G. Spivak, M. C. Johnson, *Science* **174**, 307 (1971).
16. A. M. Treisman and G. Gelade, *Cog. Psychol.* **12**, 97 (1980).
17. The experiments described herein were submitted by E.W. in partial fulfillment of the requirements for the Ph.D. degree from New York University. The experimental work was performed at the Human Information Processing Laboratory, New York University, supported by U.S. Air Force Office of Scientific Research, Life Science Directorate, grant 85-0364.

7 May 1987; accepted 8 September 1987

Mechanism of the Body-Centered Cubic–Hexagonal Close-Packed Phase Transition in Iron

W. A. BASSETT AND E. HUANG

The transition from body-centered cubic to hexagonal close-packed phase in iron has been studied in a diamond anvil cell with synchrotron radiation. The hexagonal close-packed phase, when it first appears, has a ratio of lattice parameters that is significantly larger than normal. This is attributed to a displacive mechanism that causes a distortion of the hexagonal close-packed structure in a body-centered cubic matrix. The hexagonal close-packed phase adjacent to a boundary with the body-centered cubic phase is stretched in the *c* direction and compressed in the *a* direction when it first forms.

AT ROOM TEMPERATURE AND ATMOSPHERIC pressure, iron has the body-centered cubic (bcc) structure. The bcc phase of iron undergoes a polymorphic transition at high pressure that was first reported by Bancroft *et al.* (*1*). The structure of the high-pressure polymorph of iron was later identified as hexagonal close-packed (hcp) (*2*). The bcc-hcp phase transition has been studied by a number of techniques since it was first recognized (*3–5*). The reported transition pressure ranges from 5 to 15 GPa (*6*). In order to explain this scatter, it is important to understand the mechanism of the phase transformation. A mechanism for the bcc-hcp phase transition in iron was proposed by Mao *et al.* (*7*). Confirmation of their mechanism, however, has had to await the new capabilities of synchrotron radiation.

The high intensity of synchrotron radiation allows us to rapidly acquire diffraction

Department of Geological Sciences, Cornell University, Ithaca, NY 14853.

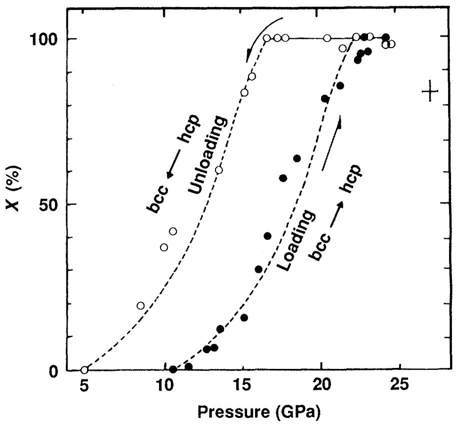

Fig. 1. The fraction of hcp iron (*X*) versus pressure at room temperature. The dashed curves are based on an empirical equation with the best fit of the data. Solid circles: data obtained in loading process; open circles: data obtained in unloading process. The error bars shown apply to all the data points.

data for the study of transient phenomena in phase transitions (*8*). This is a powerful technique for studying samples under high pressure in which the quantity of the sample is small and the high-pressure phase is not quenchable.

The experiment was carried out at the Cornell High Energy Synchrotron Source (CHESS). Broad-band radiation was used in the energy-dispersive x-ray diffraction (EDXRD) method to study the phase transition in a diamond cell (*6, 9*). An intrinsic germanium detector was used to collect the diffracted signals at a fixed angle, 2θ, from the direct beam, which was parallel to the load axis of the diamond cell. The sample used was a mixture of polycrystalline iron (Alfa Products, catalog number 400020) and gold powder (Alfa Products, catalog number 00767). Gold was used as pressure calibrant (*10*). Pressure could be gradually increased by remote-control devices. A diffraction pattern was recorded each time after the pressure was adjusted. When the transition was completed, the pressure was then decreased to atmospheric pressure. In this report, the processes of increasing and decreasing pressure are called the loading and unloading processes, respectively. Pressure was adjusted over a period of 2 minutes, and each diffraction pattern required a collection period of 2 minutes. The detailed experimental setup and methods for the study of the bcc-hcp phase transition in iron by synchrotron radiation have been described in a previous paper (*6*).

In the loading process, the phase transition started between 10.3 and 11.3 GPa. Continued increases in pressure caused increases in the ratio of the amount of hcp phase to the amount of bcc phase. The bcc phase was eliminated, and only the hcp phase remained at a pressure of more than 21 GPa. During unloading, the bcc phase reappeared between 16.3 and 15.4 GPa and the ratio of the amount of hcp phase to the amount of bcc phase decreased with further unloading. The hcp phase disappeared below 3 GPa.

When the ratios of the amount of the hcp phase and the amount of the bcc phase are plotted against pressure, we observe a hysteresis loop with a width on the order of 6 GPa (Fig. 1). This loop is similar to the observation revealed by resistance measurements (*11*), although there is a difference in the onset pressure of the transition. The hysteresis loop is characteristic of a martensitic phase transition, which takes place as temperature is increased and decreased (*12*). In the bcc-hcp phase transition in iron, the high-pressure phase appears rapidly with increasing pressure. However, if the pressure increase is halted, the ratio of hcp to bcc phase remains essentially constant. When the pressure is decreased, the hcp phase transforms back to the bcc phase and a similar pressure dependence of the transition is seen (Fig. 1). Hence, a martensitic-type of transformation in the bcc-hcp phase transition is confirmed in accordance with that suggested by Giles *et al.* (*13*).

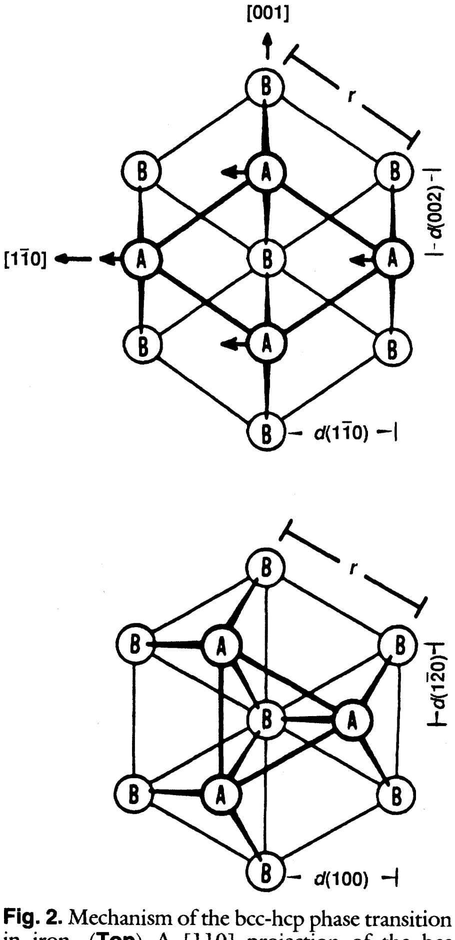

Fig. 2. Mechanism of the bcc-hcp phase transition in iron. (**Top**) A [110] projection of the bcc phase. (**Bottom**) A [001] projection of the hcp phase. Only two layers (A and B) are shown in the diagram. The bcc phase is transformed to the hcp phase by compression along the [001] and shearing of the A layer along [1$\bar{1}$0].

Table 1. Crystallographic relationship between bcc and hcp phases during phase transition.

bcc ⇒ hcp	*d* spacing	Elastic strain in hcp
(002) ⇒ (1$\bar{2}$0)	Decreases	Stretched
(1$\bar{1}$0) ⇒ (100)	Increases	Compressed
(110) ⇒ (002)	Unchanged	

The martensitic-type of transformation is termed diffusionless because it does not involve movement of atoms over distances larger than the lattice dimensions (*14*). This type of phase transformation is also termed displacive (*15*). It was pointed out by Mao *et al.* (*7*) that the hcp structure can be derived from the bcc structure through a relatively minor distortion of the bcc structure shown in Fig. 2. The hcp structure (Fig. 2, bottom) can be derived from the bcc structure (Fig. 2, top) by (i) compressing along the [001] direction of the bcc crystals, thus reducing the *d* spacing of the bcc (002) plane to form the hcp (1$\bar{2}$0) plane and expanding the *d* spacing of the bcc (110) plane to form the hcp (100) plane; (ii) translation of alternate bcc (110) layers in the [1$\bar{1}$0] direction, producing the hcp (101) reflection; and (iii) preserving the two-layer (A and B) repeat distance in the bcc structure, that is, keeping the *d* spacing of the bcc (110) plane equal to that of the hcp (002) plane. The crystallographic relationships between the bcc and hcp phases of iron during the phase transformations are given in Table 1.

A plot of the lattice parameters (*a* and *c*) of the hcp phase versus pressure reveals an anomalous pattern (Fig. 3). We observe that in the loading process the lattice parameters of the hcp phase are distorted in the pressure interval where the hcp phase first appears and coexists with the bcc phase. The *a*-axis dimension is anomalously small when compared with the *a*-axis dimension of the hcp phase at higher pressures after the bcc phase has disappeared or become a minor portion of the mixture. The *c*-axis dimension is anomalously large when compared with the hcp phase at higher pressure. In other words, the *c* axis is stretched and the *a* axis is compressed during the phase transition giving an anomaly in the *c*/*a* ratio (Fig. 3).

In the unloading process, the *c*-axis and *a*-axis dimensions of the hcp phase gradually increase in a normal fashion with decreasing pressure and the *c*/*a* ratio remains essentially constant (Fig. 3). However, when the transition to the bcc phase begins, the *c* and *a* axes once again become distorted, whereas

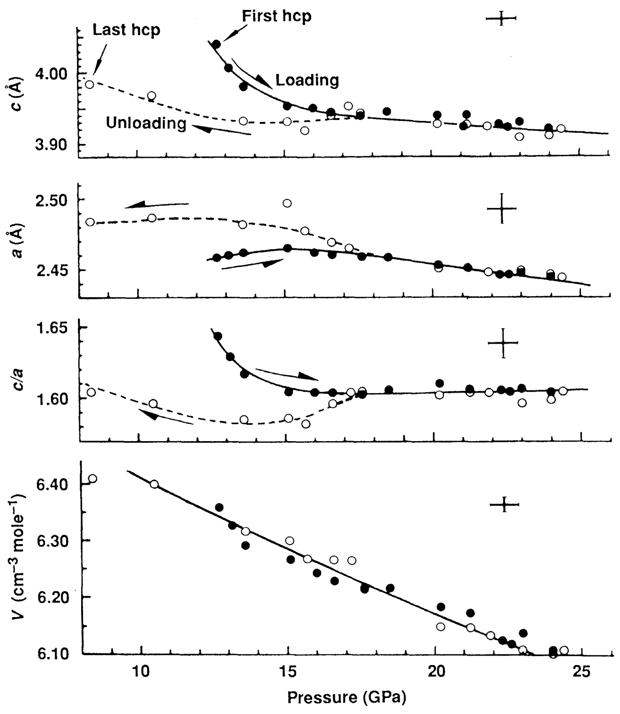

Fig. 3. The lattice parameters (c and a), c/a ratio, and molar volume (V) of the hcp iron versus pressure in the loading and unloading processes at 25°C. The error bars apply to all the data points in the plot where they appear.

the bcc and hcp phases continue to coexist. The c-axis dimension ceases to increase with decreasing load and the a-axis dimension starts to increase more rapidly. As a result the c/a ratio shows a pronounced departure from the nearly constant value it had (*16*) when the hcp phase was predominant.

The anomalous behavior of c, a, and the c/a ratio in the hcp phase is only seen in the pressure interval where the amount of the hcp phase is relatively small. The hcp phase in this stage is apparently distorted as a result of the constraint of the surrounding bcc phase. When the amount of the hcp phase is large, it is not constrained by the bcc phase and the lattice parameters of the hcp phase have normal values (Fig. 3).

In a nonhydrostatic medium, the bcc phase is most easily transformed to the hcp phase by compressing along the bcc [001] direction (Fig. 4). At the onset of the phase transition, the hcp phase grows epitaxially in the matrix of the bcc phase because of the crystallographic relationship of the two phases. If bcc and hcp occur as intimately mixed phases with an epitaxial relationship between them, then each phase is expected to be subjected to a stress imposed on it by the other phase. As a result, each phase is expected to be elastically deformed with respect to what it would be if the other phase were absent. In cases where there is a decrease in the d spacing as a result of the phase transition [such as $d(002)$ in the bcc phase], the bcc dimension is compressed but the corresponding hcp dimension [$d(1\bar{2}0)$] is stretched by the larger lattice dimension [$d(002)$] of the bcc matrix. Similarly, in cases where there is an increase in the d spacing during the phase transition, the hcp dimension is compressed as a result of the presence of the bcc matrix (Table 1).

These effects are not observable in powder diffraction patterns of the bcc phase because of its high symmetry. Some of the reflections should split because they are produced by planes that experience both stretching and compression. The x-ray diffraction method we used lacks the resolution to show this. In the case of the hexagonal phase, however, the stretching and compression occur to planes having different d spacings. According to Table 1, the hcp ($1\bar{2}0$) should be stretched and the hcp (100) should be compressed.

For the determination of the lattice parameters of the hcp phase, the diffraction patterns were collected with the x-ray beam parallel to the load axis and the detector at $2\theta = 11°$. Therefore, the lattice planes that produced the peaks in this diffraction pattern were inclined at a θ angle of only 5.5° with respect to the load axis. Hence the hcp (100) planes observed during the synchrotron experiment are those that belong to the crystallites formed by the mechanism of compressing along the bcc [001] direction as shown in Fig. 4. In this case the x-ray beam detects the compressed hcp $d(100)$ as the hcp phase grows epitaxially in the bcc matrix according to Table 1. This explains the anomalously small a-axis dimension observed in the first appearance of the hcp phase in Fig. 3.

There are two possible explanations for the anomalously large c-axis dimension. First, it may be large when the a-axis dimension is small as a result of Poisson's effect. However, this effect is probably very small. Second, the c-axis dimension may be large when the a-axis dimension is small because the (101) peak used to calculate it was produced by a set of crystallites different from the crystallites that produced the (100) peak. In this case the (101) peak may not be anomalous. Instead, the anomalously large c-axis dimension was obtained from the calculation that is based on the anomalously small a-axis dimension. The anomalous distortion that is expected from the mechanism of shortening of the $d(1\bar{2}0)$ was not observed because the crystallites are not properly oriented to produce the diffraction peak in the geometry of the synchrotron experiment.

The anomalous behavior of the lattice parameters in the hcp phase during the unloading process (Fig. 3) can be explained by an epitaxial relation between the hcp and newly formed bcc phase, which is similar to the effect observed during the loading process. The stress in a sample during unloading is not simply the reverse of the stress during loading. As the diamond anvils move apart, the sample extrudes laterally from between the anvil faces. Thus there is extension perpendicular to the load axis. It is this extension that is expected to promote the hcp-bcc transition. The crystallographic planes that should be most responsive to extension are from hcp ($1\bar{2}0$) to bcc (002) (Table 1). Because the direction of extension is perpendicular to the load axis, the extended planes should be oriented parallel to the load axis. Thus they are the planes that are best oriented to reflect the x-rays in the geometry of synchrotron experiment. If the newly formed bcc phase has an epitaxial relationship with the hcp phase, it will have the effect of stretching these planes. Because the hcp ($1\bar{2}0$) planes are the ones that are

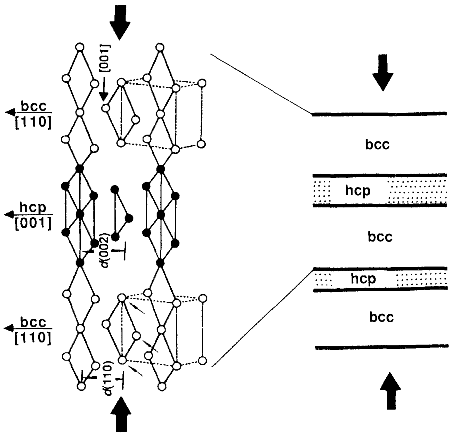

Fig. 4. Crystallographic relationship between the bcc and hcp iron showing the epitaxial growth mechanism for the phase transition. The heavy arrows represent direction of loading axis.

expected to be the most responsive to this extension, the $(1\bar{2}0)$ planes and thus the a axis should show the greatest stretching. This is consistent with the observations shown in Fig. 3.

The wide range of transition pressures reported in the literature for the bcc-hcp phase transition is attributable to the presence of anisotropic stress in the pressure cell and the orientation effect of the sample under pressure. In iron, the transition from the bcc to the hcp phase is always favored when the stress is applied in the direction parallel to the a axis of the bcc phase and when there is a shear movement along the $[1\bar{1}0]$ direction of bcc (Fig. 2). When a polycrystalline sample is compressed in a diamond anvil cell, it is likely that crystals with favorable orientation transform at pressure lower than crystals with unfavorable orientations. Thus one might find that the transition takes place at different "pressures."

The distortion of the phases in our experiment was observed in a nonhydrostatic condition where there were orientation effects arising from the presence of anisotropic stress. Using techniques similar to ours, Mao *et al.* (*7*) did not observe the anomalous lattice parameters that we did. We attribute this to some basic differences in procedure. Probably the most important difference is the method used to calculate the lattice parameters. Mao *et al.* used as many reflections as they could to calculate each lattice parameter. This had the effect of averaging out disparities resulting from lattice distortion. In our experiment we used only two reflections for calculating lattice parameters. Additional reflections that we might have used were either too weak or suffered from overlapping other reflections. The use of only two reflections greatly increased our chance of seeing the effect of lattice distortion. Another difference between the procedure followed by us and by Mao *et al.* is the time involved in collecting the data. We increased pressure and collected data points every few minutes. Mao *et al.* collected data at the rate of one point every few hundred hours. Our more rapid rate of pressure increase may have favored the martensitic-type of mechanism and the lattice distortion caused by epitaxial relationship between the phases.

In a compression study on iron, Jephcoat *et al.* (*17*) reported an anomalous compression reading in hcp iron. They found that the hcp phase has a very large a parameter and a normal c parameter, which results in an anomalously large molar volume for the hcp phase at 13.2 GPa where bcc and hcp phases coexisted. The c/a ratio was observed to be lower than the normal value in the initial stage of the phase transition (13 to 20 GPa) [see figure 4 in (*17*)]. The presence of this anomaly implies that the distorted phase can exist even under hydrostatic conditions. The nature of the anomaly, however, is apparently different as would be expected if the anisotropic stress is absent.

The explanation for this lies in the mechanism of volume reduction that takes place during the bcc-hcp phase transition. There is essentially no dimensional change between $d(110)$ of bcc and $d(002)$ of hcp phase (Table 1). Thus the c-axis dimension of the hcp phase experiences no stretching or compression even if it is constrained by an epitaxial relationship with the bcc phase. On the other hand, there is both decrease and increase in dimensions perpendicular to the c axis. There must, however, be a net decrease in dimension perpendicular to the c axis to account for the large volume change during the bcc-hcp phase transition. If this decrease in dimension is constrained by an epitaxial relationship between hcp and bcc phases, then the a axes of the newly formed hcp phase must on average be stretched compared with the dimensions they would have in the absence of the bcc phase. This effect does not depend on anisotropic stress or x-ray geometry and should be observable under completely isotropic conditions.

REFERENCES AND NOTES

1. D. Bancroft, E. L. Peterson, S. Minshall, *J. Appl. Phys.* **27**, 291 (1956).
2. J. C. Jamieson and A. W. Lawson, *ibid.* **33**, 776 (1962).
3. P. C. Johnson, B. A. Stein, R. S. Davis, *ibid.*, p. 557.
4. T. Takahashi and W. A. Bassett, *Science* **145**, 483 (1964).
5. F. P. Bundy, *J. Appl. Phys.* **36**, 616 (1965).
6. E. Huang *et al.*, in *High-Pressure Research in Mineral Physics*, M. H. Manghnani and Y. Syono, Eds. (Scientific Publishing, Tokyo, in press).
7. H. K. Mao, W. A. Bassett, T. Takahashi, *J. Appl. Phys.* **38**, 272 (1967).
8. B. Buras, J. Staun Olsen, L. Gerward, G. Will, E. Hinze, *J. Appl. Crystallogr.* **10**, 431 (1977).
9. M. D. Furnish and W. A. Bassett, *J. Geophys. Res.* **88**, 10333 (1983).
10. D. L. Heinz and R. Jeanloz, *J. Appl. Phys.* **55**, 885 (1984).
11. A. L. F. Vereshchagin *et al.*, *Dokl. Akad. Nauk. SSSR* **185**, 785 (1969).
12. P. G. Shewman, *Transformation in Metals* (McGraw-Hill, New York, 1969).
13. P. M. Giles, M. H. Longenbach, A. R. Marder, *J. Appl. Phys.* **42**, 4290 (1971).
14. J. W. Christian, *The Theory of Transformations in Metals and Alloys*, vol. 1, *Equilibrium and General Kinetic Theory* (Pergamon, Oxford, 1975).
15. A. G. Khachaturyan, *Theory of Structural Transformations in Solids* (Wiley, New York, 1983).
16. E. Huang *et al.*, *J. Geophys. Res.* **92**, 8129 (1987).
17. A. P. Jephcoat *et al.*, *ibid.* **91**, 4677 (1986).

6 July 1987; accepted 8 September 1987

In Situ X-ray Absorption Study of Surface Complexes: Selenium Oxyanions on α-FeOOH

KIM F. HAYES, A. LAWRENCE ROE, GORDON E. BROWN, JR.,
KEITH O. HODGSON, JAMES O. LECKIE, GEORGE A. PARKS

A novel application of x-ray absorption spectroscopy has provided structural information for ions sorbed at oxide-water interfaces. As an example, in situ extended x-ray absorption fine structure (EXAFS) measurements of adsorbed selenate and selenite ions at an α-FeOOH(goethite)–water interface have been performed; these measurements show that selenate forms a weakly bonded, outer-sphere complex and that selenite forms a strongly bonded, inner-sphere complex. The selenite ion is bonded directly to the goethite surface in a bidentate fashion with two iron atoms 3.38 angstroms from the selenium atom. Adsorbed selenate has no iron atom in the second coordination shell of selenium, which indicates retention of its hydration sphere upon sorption. This method provides direct structural information for adsorbed species at solid-liquid interfaces.

THE PARTITIONING OF IONS AT INTERFACES between solids and liquids is poorly understood at the molecular level, yet detailed structural information on surface complexes is essential for quantitative description of many interfacial processes. These processes play a fundamental role in a variety of fields, including geochemistry (ore deposition, metal extraction, and weathering), electrical engineering (ion-sensitive field effect transistors), catalysis (doping of oxide supports), oceanography (scavenging of trace metals), environmental engineering (removal of trace contaminants from industrial waste waters or ground water), and material science (corrosion control).

Most spectroscopic methods that are commonly used to probe interfaces require that the sample be dried and placed under high-vacuum conditions. For example, x-ray

---

K. F. Hayes and J. O. Leckie, Department of Civil Engineering, Stanford University, Stanford, CA 94305.
A. L. Roe and K. O. Hodgson, Department of Chemistry, Stanford University, Stanford, CA 94305.
G. E. Brown, Jr., and G. A. Parks, School of Earth Sciences, Stanford University, Stanford, CA 94305.